

# Study of Radiative Leptonic $D$ Meson Decays

C. Q. Geng<sup>a</sup>, C. C. Lih<sup>a</sup> and Wei-Min Zhang<sup>b</sup>

<sup>a</sup>*Department of Physics, National Tsing Hua University  
Hsinchu, Taiwan, Republic of China*

and

<sup>b</sup>*Department of Physics, National Cheng Kung University  
Tainan, Taiwan, Republic of China*

## Abstract

We study the radiative leptonic  $D$  meson decays of  $D_{(s)}^+ \rightarrow l^+ \nu_l \gamma$  ( $l = e, \mu, \tau$ ),  $D^0 \rightarrow \nu \bar{\nu} \gamma$  and  $D^0 \rightarrow l^+ l^- \gamma$  ( $l = e, \mu$ ) within the light front quark model. In the standard model, we find that the decay branching ratios of  $D_{(s)}^+ \rightarrow e^+ \nu_e \gamma$ ,  $D_{(s)}^+ \rightarrow \mu^+ \nu_\mu \gamma$  and  $D_{(s)}^+ \rightarrow \tau^+ \nu_\tau \gamma$  are  $6.9 \times 10^{-6}$  ( $7.7 \times 10^{-5}$ ),  $2.5 \times 10^{-5}$  ( $2.6 \times 10^{-4}$ ), and  $6.0 \times 10^{-6}$  ( $3.2 \times 10^{-4}$ ), and that of  $D^0 \rightarrow l^+ l^- \gamma$  ( $l = e, \mu$ ) and  $D^0 \rightarrow \nu \bar{\nu} \gamma$  are  $6.3 \times 10^{-11}$  and  $2.7 \times 10^{-16}$ , respectively.

# 1 Introduction

In the standard model, flavor changing neutral current (FCNC) decays of  $D$  mesons are predicted to be very rare. Such processes are forbidden at the tree level but can occur at higher loop level. On the other hand, these rare decays make a good chance to probe for new physics [1]. Recently, the new experimental limits with the range  $10^{-4}$  to  $10^{-5}$  for FCNC decays of the charm mesons were obtained at Fermilab E791, E771 and CLEO II [2, 3, 4].

As we known, the two-body leptonic decays of  $D$  mesons of  $D \rightarrow l_i \bar{l}_j$  ( $l_{i,j} = e, \mu, \nu$ ) are helicity suppressed. Explicitly, in the standard model, the decay branching ratios of  $D_{(s)}^+ \rightarrow e^+ \nu_e$ ,  $\mu^+ \nu_\mu$ ,  $\tau^+ \nu_\tau$  and  $D^0 \rightarrow l^+ l^-$  are  $1.0 \times 10^{-8}$  ( $9.5 \times 10^{-8}$ ),  $4.7 \times 10^{-4}$  ( $9.5 \times 10^{-3}$ ),  $1.2 \times 10^{-3}$  ( $4.2 \times 10^{-2}$ ) and  $O(10^{-19})$ , respectively, while that of  $D^0 \rightarrow \nu \bar{\nu}$  is zero. It is clear that the rates for the modes of  $D \rightarrow l_i \bar{l}_i$  ( $l_i = e, \mu, \nu$ ) are too small to be measured due to the helicity suppression as well as Glashow-Iliopoulos-Maiani (GIM) mechanism effect [5].

To avoid the helicity suppression, we will consider three body decays such as  $D^+ \rightarrow l^+ \nu_l \gamma$  and  $D^0 \rightarrow l^+ l^- \gamma$  with a photon radiated from charged particles. The amplitudes of the decays can be divided into the “internal-bremsstrahlung” (IB) parts and the “structure-dependent” (SD) parts. Since the photon is emission from the external charged leptons, IB parts are still helicity suppressed for the light charged lepton modes, while in SD one of the photon is emitted from intermediate states that they are free of the helicity suppression. Therefore, the decay rates of  $D^+ \rightarrow l^+ \nu_l \gamma$  and  $D^0 \rightarrow l^+ l^- \gamma$  ( $l = e, \mu$ ) might have an enhancement with respect to the purely leptonic modes of  $D^+ \rightarrow l^+ \nu_l$  and  $D^0 \rightarrow l^+ l^-$ , respectively.

It has been pointed out that the heavy flavor decays can be analyzed with the help of heavy quark effective theory. For charmed decays, this is questioned since the charm quark mass is not much larger than the QCD scale. Therefore, we will use the light front quark model [6, 7, 8, 9, 10, 11] to evaluate the hadronic matrix elements in  $D \rightarrow \gamma$  transitions. These decay modes have been studied in various models [12, 13, 14]. It is known that as the recoil momentum increases, we have to start considering relativistic effects seriously. The light front quark model [7] is the widely accepted relativistic quark model in which a consistent and relativistic treatment of quark spins and the center-of-mass motion can be carried out. In this work, we calculate form factors in  $D \rightarrow \gamma$  directly at time-like momentum transfers by using the relativistic light-front hadronic wave

function. The parameters in the wave function are determined from Refs. [7, 8, 9]. Within the framework of light-front quark model for decay processes, one may calculate hadronic matrix elements in the frame where the transfer momentum is purely longitudinal, *i.e.*,  $p_\perp = 0$  and  $p^2 = p^+p^-$ , which covers the entire range of the momentum transfers. We will give their the momentum dependence in whole kinematics region of  $0 \leq p^2 \leq p_{\max}^2$ .

The paper is organized as follows. In Sec. 2, we study the form factors of  $D \rightarrow \gamma$  transitions within the light front framework. We present the decay amplitudes and calculate the decay branching ratios of  $D_{(s)}^+ \rightarrow l^+ \nu_l \gamma$ ,  $D^0 \rightarrow \nu \bar{\nu} \gamma$  and  $D^0 \rightarrow l^+ l^- \gamma$  in Sec. 3, 4 and 5, respectively. In Sec. 6, the conclusion is given.

## 2 Form factors of $D \rightarrow \gamma$ transitions

To evaluate the  $D_u \rightarrow \gamma$  transition, one needs to consider the following currents:

$$\begin{aligned} J^\mu &= \bar{u} \gamma^\mu (1 - \gamma_5) c \\ T^\mu &= \bar{u} i \sigma^{\mu\nu} p_\nu (1 + \gamma_5) c, \end{aligned} \quad (1)$$

where  $p$  is the momentum transform,  $D_u = \bar{u}c$  and  $u$  stands for the light quark such as a d-quark or u-quark or s-quark so that  $D_d \equiv D^+$ ,  $D_u \equiv D^0$  and  $D_s \equiv D_s^+$ , respectively. Our main task is to calculate the hadronic matrix elements for  $D \rightarrow \gamma$  transitions, which can be parametrized as:

$$\begin{aligned} \langle \gamma(q_\gamma) | \bar{u} \gamma_\mu \gamma_5 c | D(p + q_\gamma) \rangle &= -e \frac{F_A}{M_D} [(p \cdot q_\gamma) \epsilon_\mu^* - (\epsilon^* \cdot p) q_{\gamma\mu}], \\ \langle \gamma(q_\gamma) | \bar{u} \gamma_\mu c | D(p + q_\gamma) \rangle &= ie \frac{F_V}{M_D} \varepsilon_{\mu\alpha\beta\nu} \epsilon^{*\alpha} p^\beta q_\gamma^\nu, \end{aligned} \quad (2)$$

$$\begin{aligned} \langle \gamma(q_\gamma) | \bar{u} i \sigma_{\mu\nu} p^\nu \gamma_5 c | D(p + q_\gamma) \rangle &= ie F_{TA} \epsilon^\nu (p \cdot q_\gamma g_{\mu\nu} - p_\nu q_{\gamma\mu}), \\ \langle \gamma(q_\gamma) | \bar{u} i \sigma_{\mu\nu} p^\nu c | D(p + q_\gamma) \rangle &= e F_{TV} \varepsilon_{\mu\beta\rho\lambda} \epsilon^\beta q_\gamma^\rho p^\lambda, \end{aligned} \quad (3)$$

where the  $\epsilon_\mu$  is the photon polarization vector,  $q_\gamma$  and  $p + q_\gamma$  are photon and  $D$  meson four momenta and  $F_A$ ,  $F_V$ ,  $F_{TA}$  and  $F_{TV}$  are the form factors of axial-vector, vector, axial-tensor and tensor, respectively.

In the light front approach, the physically accessible kinematics region is  $0 \leq p^2 \leq p_{\max}^2 = M_D^2$  due to the time-like momentum transfers. The  $D_u$  meson bound state in light-front quark model consists of an anti-quark  $\bar{u}$  and a quark  $c$  with the total momentum

$(p + q_\gamma)$ . It can be expressed by:

$$|D(p + q_\gamma) > = \sum_{\lambda_1 \lambda_2} \int [dk_1][dk_2] 2(2\pi)^3 \delta^3(p + q_\gamma - k_1 - k_2) \\ \times \Phi_D^{\lambda_1 \lambda_2}(x, k_\perp) b_{\bar{u}}^+(k_1, \lambda_1) d_c^+(k_2, \lambda_2) |0 >, \quad (4)$$

where  $k_{1(2)}$  is the on-mass shell light front momentum of the internal quark  $\bar{u}(c)$ , the light front relative momentum variables  $(x, k_\perp)$  are defined by

$$k_1^+ = x(p + q_\gamma)^+, \quad k_{1\perp} = x(p + q_\gamma)_\perp + k_\perp, \quad (5)$$

and

$$\Phi_D^{\lambda_1 \lambda_2}(x, k_\perp) = \left( \frac{2k_1^+ k_2^+}{M_0^2 - (m_u - m_b)^2} \right)^{\frac{1}{2}} \bar{u}(k_1, \lambda_1) \gamma^5 v(k_2, \lambda_2) \phi(x, k_\perp), \quad (6)$$

with  $\phi(x, k_\perp)$  being the momentum distribution amplitude. The amplitude of  $\phi(x, k_\perp)$  can be solved in principles by the light-front QCD bound state equation [7, 8, 9]. However, we use the Gaussian type wave function:

$$\phi(x, k_\perp) = N \sqrt{\frac{dk_z}{dx}} \exp \left( -\frac{\vec{k}_\perp^2}{2\omega_D^2} \right), \quad (7)$$

where

$$[dk_1] = \frac{dk^+ dk_\perp}{2(2\pi)^3}, \quad N = 4 \left( \frac{\pi}{\omega_D^2} \right)^{\frac{3}{4}}, \\ k_z = \left( x - \frac{1}{2} \right) M_0 + \frac{m_c^2 - m_u^2}{2M_0}, \quad M_0^2 = \frac{k_\perp^2 + m_c^2}{x} + \frac{k_\perp^2 + m_u^2}{1-x}, \\ \sum_\lambda u(k, \lambda) \bar{u}(k, \lambda) = \frac{m + \not{k}}{k^+}, \quad \sum_\lambda v(k, \lambda) \bar{v}(k, \lambda) = -\frac{m - \not{k}}{k^+}. \quad (8)$$

For the gauged photon state, one has: [15]

$$|\gamma(q_\gamma) > = N' \left\{ a^+(q_\gamma, \lambda) + \sum_{\lambda_1 \lambda_2} \int [dk_1][dk_2] 2(2\pi)^3 \delta^3(q_\gamma - k_1 - k_2) \right. \\ \left. \times \Phi_{q\bar{q}}^{\lambda_1 \lambda_2 \lambda}(q_\gamma, k_1, k_2) b_q^+(k_1, \lambda_1) d_{\bar{q}}^+(k_2, \lambda_2) \right\} |0 >, \quad (9)$$

where

$$\Phi_{q\bar{q}}^{\lambda_3 \lambda_4 \lambda}(q_\gamma, k_1, k_2) = \frac{e_q}{ED} \chi_{-\lambda_2}^+ \left\{ -2 \frac{q_\perp \cdot \epsilon_\perp}{q^+} - \gamma_\perp \cdot \epsilon_\perp \frac{\gamma_\perp \cdot k_{2\perp} - m_2}{k_2^+} \right. \\ \left. - \frac{\gamma_\perp \cdot k_{1\perp} - m_1}{k_1^+} \gamma_\perp \cdot \epsilon_\perp \right\} \chi_{\lambda_1}, \quad (10)$$

with

$$ED = \frac{q_{\gamma\perp}^2}{q_\gamma^+} - \frac{k_{1\perp}^2 + m_1^2}{k_1^+} - \frac{k_{2\perp}^2 + m_2^2}{k_2^+}. \quad (11)$$

To calculate the matrix elements of the Eqs. (2) and (3), we choose a frame with the transverse momentum  $p_\perp = 0$ . The  $p^2 = p^+p^- \geq 0$  covers the entire range of the momentum transfers. By considering the “good” component  $\mu = +$ , the hadronic matrix elements of Eqs. (2) and (3) can be rewritten as:

$$\begin{aligned} \langle \gamma(q_\gamma) | u_+^+ \gamma_5 c_+ | D(p + q_\gamma) \rangle &= -ie \frac{F_A}{2M_D} (\epsilon_\perp^* \cdot q_{\gamma\perp}) p^+, \\ \langle \gamma(q_\gamma) | u_+^+ c_+ | D(p + q_\gamma) \rangle &= e \frac{F_V}{2M_D} \epsilon^{ij} \epsilon_i^* q_{\gamma j} p^+, \end{aligned} \quad (12)$$

and

$$\begin{aligned} \langle \gamma(q_\gamma) | (u_+^+ \gamma^0 \gamma_5 c_- - u_-^+ \gamma^0 \gamma_5 c_+) | D(p + q_\gamma) \rangle &= e F_{TA} (\epsilon_\perp^* \cdot q_{\gamma\perp}), \\ \langle \gamma(q_\gamma) | (u_+^+ \gamma^0 c_- - u_-^+ \gamma^0 c_+) | D(p + q_\gamma) \rangle &= -ie F_{TV} \epsilon^{ij} \epsilon_i^* q_{\gamma j}, \end{aligned} \quad (13)$$

where  $u_+(c_+)$  and  $u_-(c_-)$  are the light-front up and down components of the quark fields, and they have the two-component forms:

$$q_+ = \begin{pmatrix} \chi \\ 0 \end{pmatrix}, \quad (14)$$

and

$$\begin{aligned} q_- &= \frac{1}{i\partial^+} (i\alpha_\perp \cdot \partial_\perp + \beta m_q) q_+ \\ &= \begin{pmatrix} 0 \\ \frac{1}{\partial^+} (\tilde{\sigma}_\perp \cdot \partial_\perp + m_q) \chi_q \end{pmatrix}, \end{aligned} \quad (15)$$

respectively.

In Eq. (15),  $\chi_q$  is a two-component spinor field and  $\sigma$  is the Pauli matrix. The form factors  $F_{V,A}$  and  $F_{TV,TA}$  in Eqs. (12) and (13) are then found to be:

$$\begin{aligned} F_A(p^2) &= -4M_D \int \frac{dx d^2 k_\perp}{2(2\pi)^3} \Phi(x', k_\perp^2) \frac{1}{1-x'} \\ &\quad \times \left\{ \frac{2}{3} \frac{m_b - B k_\perp^2 \Theta}{m_c^2 + k_\perp^2} - \frac{2}{3} \frac{m_u - A k_\perp^2 \Theta}{m_u^2 + k_\perp^2} \right\}, \end{aligned} \quad (16)$$

$$\begin{aligned} F_V(p^2) &= 4M_D \int \frac{dx d^2 k_\perp}{2(2\pi)^3} \Phi(x', k_\perp^2) \frac{1}{1-x'} \\ &\quad \left\{ \frac{2}{3} \frac{m_c + (1-x')(m_c - m_u) k_\perp^2 \Theta}{m_c^2 + k_\perp^2} + \frac{2}{3} \frac{m_u - x'(m_c - m_u) k_\perp^2 \Theta}{m_u^2 + k_\perp^2} \right\}, \end{aligned} \quad (17)$$

$$F_{TA}(p^2) = \int \frac{dx d^2 k_{\perp}}{2(2\pi)^3} \Phi(x', k_{\perp}^2) \times \left\{ \frac{2}{3} \frac{A_1 + A_2 k_{\perp}^2 \Theta}{m_c^2 + k_{\perp}^2} + \frac{2}{3} \frac{B_1 + B_2 k_{\perp}^2 \Theta}{m_u^2 + k_{\perp}^2} \right\}, \quad (18)$$

$$F_{TV}(p^2) = - \int \frac{dx d^2 k_{\perp}}{2(2\pi)^3} \Phi(x', k_{\perp}^2) \times \left\{ \frac{2}{3} \frac{C_1 + C_2 k_{\perp}^2 \Theta}{m_c^2 + k_{\perp}^2} + \frac{2}{3} \frac{D_1 + D_2 k_{\perp}^2 \Theta}{m_u^2 + k_{\perp}^2} \right\}, \quad (19)$$

where

$$\begin{aligned} A &= (1-2x)x'(m_c - m_u) - 2xm_u, \\ B &= 2(1-x)x'm_c + (1-2x)(1-x')m_u, \\ A_1 &= \frac{2}{xx'^2(1-x')(1-x)} \left\{ (x' + x - 2x'x) [x'(x-1) - x(2x-1)] k_{\perp}^2 \right. \\ &\quad \left. + x[(x-x') + 2x'x(1-x)] m_c^2 + 2x^2(1-x')^2 m_c m_u \right\}, \\ A_2 &= \frac{2(x-x')}{xx'^2(1-x')(1-x)} \left\{ (x' + x - 2x'x)(1-2x)k_{\perp}^2 \right. \\ &\quad \left. + 2x(1-x')m_u m_c - x(1-2x)(1-x')^2 m_u^2 + x'(1+x'x - 2xx'^2) m_c^2 \right\}, \\ B_1 &= \frac{2}{x'x(1-x)(1-x')^2} \left\{ (x' + x - 2x'x)(1-2x + 2x^2 - x'x)k_{\perp}^2 \right. \\ &\quad \left. + 2xx'(1-x')(1-x)m_u m_c + (1-x')(x' + x - 4x'x + 2x'x^2) m_u^2 \right\}, \\ B_2 &= \frac{2(x-x')}{x'x(1-x)(1-x')^2} \left\{ -(x' + x - 2x'x)(1-2x)k_{\perp}^2 \right. \\ &\quad \left. - [(1-2x)x'^2(1-x)m_c^2 + (1-x')(x' + x - 3x'x - 2x^2(1-x')) m_u^2] \right\}, \\ C_1 &= \frac{2}{xx'^2(1-x')(1-x)} \left\{ (x - x' + xx')(x' + x - 2x'x)k_{\perp}^2 \right. \\ &\quad \left. - 2x^2(1-x')^2 m_c m_u + x'[(x-x') - 2(1-x')x^2] m_c^2 \right\}, \\ C_2 &= \frac{2(x-x')}{xx'^2(1-x')(1-x)} \left\{ (x' + x - 2x'x)k_{\perp}^2 + x'(1-2x + xx') m_c^2 \right. \\ &\quad \left. - m_q^2 x(1-x')^2 - 2x(1-x')m_u m_c \right\}, \\ D_1 &= \frac{2}{x(1-x)x'(1-x')^2} \left\{ -(1-x)(1-2x+x')(x' + x - 2x'x)k_{\perp}^2 \right. \\ &\quad \left. - [(1-x')(x' + x - 2x^2 - 2x'x + 2x^2 x') m_u^2 + 2x'^2(1-x)^2 m_u m_c] \right\}, \end{aligned}$$

$$\begin{aligned}
D_2 &= \frac{2(x-x')}{x'(1-x)x(1-x')^2} \left\{ (x' + x - 2x'x)k_\perp^2 + x'^2(1-x)m_c^2 \right. \\
&\quad \left. + (1-x')(x' - x - x'x)m_u^2 \right\}, \\
\Phi(x, k_\perp^2) &= N \left( \frac{2x(1-x)}{M_0^2 - (m_u - m_c)^2} \right)^{1/2} \sqrt{\frac{dk_z}{dx}} \exp \left( -\frac{\vec{k}^2}{2\omega_D^2} \right), \\
\Theta &= \frac{1}{\Phi(x, k_\perp^2)} \frac{d\Phi(x, k_\perp^2)}{dk_\perp^2}, \\
x' &= x \left( 1 - \frac{p^2}{M_D^2} \right), \quad \vec{k} = (\vec{k}_\perp, \vec{k}_z).
\end{aligned} \tag{20}$$

To illustrate numerical results, we input  $m_u = 0.3$ ,  $m_c = 1.4$ , and  $\omega = 0.5$  in  $GeV$ . The form factors of  $F_{V,A}$  and  $F_{TV,TA}$  are shown in Figures 1 and 2, respectively.

### 3 $D_{(s)}^+ \rightarrow l^+ \nu_l \gamma$

#### 3.1 Matrix elements and kinematics

In this work, we investigate the decays of  $D_q^+ \rightarrow l^+ \nu_l \gamma$  ( $q = d, s$ ). The effective Hamiltonian for  $c \rightarrow q l \nu_l$  at the quark level in the standard model has been obtained by using similar results for  $b \rightarrow q l \nu_l$

$$H_{eff}(c \rightarrow q l \nu_l) = \frac{G_F}{\sqrt{2}} V_{cq} \bar{q} \gamma_\mu (1 - \gamma_5) c \bar{\nu}_l \gamma_\mu (1 - \gamma_5) l. \tag{21}$$

From Eq. (21), due to the emissions of real photons that the decay amplitude of  $D_q^+ \rightarrow l^+ \nu_l \gamma$  can be written as

$$M = M_{IB} + M_{SD}, \tag{22}$$

$$M_{IB} = i \frac{G_F}{\sqrt{2}} V_{cq} f_D m_l \epsilon_\mu^* D^\mu, \tag{23}$$

$$M_{SD} = -i \frac{G_F}{\sqrt{2}} V_{cq} \epsilon_\alpha L_\beta H^{\alpha\beta}, \tag{24}$$

where  $M_{IB}$  and  $M_{SD}$  represent the amplitudes from the IB and SD contributions, respectively, and

$$D^\mu = \bar{u}(p_\nu)(1 + \gamma_5) \left( \frac{p^\mu}{p \cdot q} - \frac{2p_l^\mu + \not{q} \gamma^\mu}{2p_l \cdot q} \right) v(p_l, s_l), \tag{25}$$

$$L_\beta = \bar{u}(p_\nu) \gamma_\beta (1 - \gamma_5) v(p_l, s_l), \tag{26}$$

$$H^{\alpha\beta} = e \frac{F_A}{M_D} (-g^{\alpha\beta} p \cdot q + p^\alpha q^\beta) + ie \frac{F_V}{M_{D_u}} \epsilon^{\alpha\beta\mu\nu} q_\mu p_\nu, \tag{27}$$

with  $f_{D(s)}$  being the  $D(s)$  decay constants,  $\epsilon_\mu$  and  $s_l$  the four vectors of the photon polarization and charged lepton, and  $p$ ,  $p_l$ ,  $p_\nu$ , and  $q$  the four momenta of  $D(s)^+$ ,  $l$ ,  $\nu$  and  $\gamma$ , respectively. The physics allowed region of  $D(s)^+ \rightarrow l^+ \nu_l \gamma$  is

$$m_l^2 \leq p^2 \leq M_{D(s)}^2. \quad (28)$$

To describe the kinematics of  $D(s)^+ \rightarrow l^+ \nu_l \gamma$ , one needs two variables, for which we define  $x_\gamma = 2E_\gamma/M_{D(s)}$  and  $y = 2E_l/M_{D(s)}$ . We write the physics region for  $x_\gamma$  and  $y$  as:

$$0 \leq x_\gamma \leq 1 - r_l, \quad (29)$$

$$1 - x_\gamma + \frac{r}{1 - x_\gamma} \leq y \leq 1 + r_l, \quad (30)$$

where

$$r_l = \frac{m_l^2}{M_D^2} = \begin{cases} 7.1 \times 10^{-8} & \text{for } l = e \\ 3.2 \times 10^{-3} & \text{for } l = \mu \\ 0.9 & \text{for } l = \tau \end{cases} \quad (31)$$

for  $D^+ \rightarrow l^+ \nu_l \gamma$  and

$$r_l = \frac{m_l^2}{M_{D_s}^2} = \begin{cases} 6.4 \times 10^{-8} & \text{for } l = e \\ 2.8 \times 10^{-3} & \text{for } l = \mu \\ 0.8 & \text{for } l = \tau \end{cases} \quad (32)$$

for  $D_s^+ \rightarrow l^+ \nu_l \gamma$ .

### 3.2 Decay rates

In the  $D_q^+$  ( $q = d$  or  $s$ ) rest frame, the partial decay rate is found by [16]

$$d\Gamma = \frac{1}{(2\pi)^3} \frac{1}{8M_{D_q}} |M|^2 dE_\gamma dE_l. \quad (33)$$

Using  $x_\gamma$  and  $y$ , from Eq. (33) we obtain the differential decay rate as

$$\frac{d^2\Gamma^l}{dx_\gamma dy} = \frac{M_D}{256\pi^3} |M|^2 = \frac{M_{D_q}}{256\pi^3} e^2 G_F^2 V_{cq}^2 (1 - \lambda) A, \quad (34)$$

and

$$A = A_{IB}(x_\gamma, y) + A_{SD}(x_\gamma, y) + A_{IN}(x_\gamma, y), \quad (35)$$

$$A_{IB}(x_\gamma, y) = \frac{4m_l^2 |f_{D_q}|^2}{\lambda x_\gamma^2} \left[ x_\gamma^2 + 2(1 - r_l) \left( 1 - x_\gamma - \frac{r_l}{\lambda} \right) \right], \quad (36)$$



$$\begin{aligned}
A_{SD}(x_\gamma, y) = & M_{D_q}^4 x_\gamma^2 \left[ |F_V + F_A|^2 \frac{\lambda^2}{1 - \lambda} \left( 1 - x_\gamma - \frac{r_l}{\lambda} \right) \right. \\
& \left. + |F_V - F_A|^2 (y - \lambda) \right], \tag{37}
\end{aligned}$$

$$\begin{aligned}
A_{IN}(x_\gamma, y) = & -4M_{D_q} m_l^2 \left[ \text{Re}[f_{D_q}(F_V + F_A)^*] \left( 1 - x_\gamma - \frac{r_l}{\lambda} \right) \right. \\
& \left. - \text{Re}[f_{D_q}(F_V - F_A)^*] \frac{1 - y + \lambda}{\lambda} \right], \tag{38}
\end{aligned}$$

where  $\lambda = (x_\gamma + y - 1 - r)/x_\gamma$ . In Figures 3 and 4, we show the differential branching ratios of  $D^+ \rightarrow \mu^+ \nu_\mu \gamma$  and  $D_s^+ \rightarrow \mu^+ \nu_\mu \gamma$  as functions of the photon energies, where we have used  $m_d = 0.3 \text{ GeV}$ ,  $m_s = 0.4 \text{ GeV}$ ,  $m_c = 1.5 \text{ GeV}$ ,  $|V_{cd}| \simeq 0.22$ ,  $|V_{cs}| \simeq 0.974$ ,  $\omega = 0.5 \text{ GeV}$ ,  $\tau_{D_s^+} \simeq 0.467 \text{ ps}$ ,  $\tau_{D^+} \simeq 1.05 \text{ ps}$  and  $f_D = f_{D_s} = 230 \text{ MeV}$  [16, 17]. We get the integrated branching ratios of  $D^+$  and  $D_s^+ \rightarrow l^+ \nu_l \gamma$  ( $l = e, \mu, \tau$ ) in Tables 1 and 2.

Table 1: Integrated branching ratios for the radiative leptonic  $D^+$  decays

Integrated Decay Branching Ratios	IB	SD	IN	Sum	Ref. [14]
$10^6 B(D^+ \rightarrow e^+ \nu_e \gamma)$	$1.0 \times 10^{-3}$	6.9	$6.2 \times 10^{-5}$	6.9	82
$10^6 B(D^+ \rightarrow \mu^+ \nu_\mu \gamma)$	17.2	6.8	$6.2 \times 10^{-1}$	24.6	—
$10^6 B(D^+ \rightarrow \tau^+ \nu_\tau \gamma)$ (Cut $\delta = 0.01$ )	5.6	$1.3 \times 10^{-6}$	$3.7 \times 10^{-1}$	6.0	—

Table 2: Integrated branching ratios for the radiative leptonic  $D_s^+$  decays

Integrated Decay Branching Ratios	IB	SD	IN	Sum	Ref. [14]	Ref. [13]
$10^5 B(D_s^+ \rightarrow e^+ \nu_e \gamma)$	$1.1 \times 10^{-3}$	7.7	$6.8 \times 10^{-5}$	7.7	90	17
$10^5 B(D_s^+ \rightarrow \mu^+ \nu_\mu \gamma)$	17.8	7.5	$7.1 \times 10^{-1}$	26.0	—	17
$10^5 B(D_s^+ \rightarrow \tau^+ \nu_\tau \gamma)$ (Cut $\delta = 0.01$ )	30.7	$1.8 \times 10^{-3}$	1.7	32.4	—	—

We now compare our results with Refs. [13, 14]. As shown in Tables 1 and 2, our result are much smaller than that in Ref. [14] but close to the values in Ref. [13]. We note that for the  $\mu$  and  $\tau$  channels the IB contributions are dominant since D-mesons are not very heavy.

## 4 $D^0 \rightarrow \nu \bar{\nu} \gamma$

### 4.1 Matrix elements and kinematics

For the processes of  $D^0 \rightarrow \nu_l \bar{\nu}_l \gamma$  ( $l = e, \mu, \tau$ ), at the quark level, they arise from the box and  $Z$ -penguin diagrams that contribute to  $c \rightarrow u \nu_l \bar{\nu}_l$  with the photon emitting from the charged particles in the diagrams. However, when the photon line is attached to the internal charge lines such as the  $W$  boson and quark lines, there is a suppression factor of  $m_c^2/M_W^2$  in the Wilson coefficient in comparing with those in  $c \rightarrow u \nu_l \bar{\nu}_l$ . Thus, we need only to consider the diagrams with the photon from the external quarks. The effective Hamiltonian for  $c \rightarrow u \nu_l \bar{\nu}_l$  is given by

$$H_{eff}(D^0 \rightarrow \nu_l \bar{\nu}_l \gamma) = \frac{G_F}{\sqrt{2}} \frac{\alpha}{2\pi \sin^2 \theta_W} \sum_{i=d,s,b} V_{ui} V_{ci}^* D(x_i) \bar{u} \gamma_\mu (1 - \gamma_5) c \bar{\nu}_l \gamma_\nu (1 - \gamma_5) \nu_l, \quad (39)$$

where

$$D(x_i) = \frac{1}{4} \left[ \frac{x_i^2 - x_i + 3}{x_i - 1} + \frac{3(x_i - 2)}{(1 - x_i)^2} x_i \ln x_i \right], \quad (40)$$

and  $x_i = m_i^2/M_W^2$  with  $m_i$  ( $i = d, s, b$ ) being the current quark masses. We note that in Eqs. (39) and (40), only the leading contributions have been included and the additional  $\alpha_s$  correction to the result, which are small [18].

### 4.2 Decay amplitude

From the effective Hamiltonian for  $c \rightarrow u \nu_l \bar{\nu}_l$  of Eq. (39) and the form factors defined in Eq. (12), we can write the amplitude of  $D^0 \rightarrow \nu_l \bar{\nu}_l \gamma$  as

$$M = -ie \frac{G_F}{\sqrt{2}} \frac{\alpha}{2\pi \sin^2 \theta_W} \sum_{i=d,s,b} V_{ui} V_{ci}^* D(x_i) \epsilon_\mu^* H^{\mu\nu} \bar{u}(p_{\bar{\nu}}) \gamma_\mu (1 - \gamma_5) v(p_\nu), \quad (41)$$

with

$$H_{\mu\nu} = \frac{F_A}{M_D} (-p \cdot q_\gamma g_{\mu\nu} + p_\mu q_{\gamma\nu}) + i \epsilon_{\mu\nu\alpha\beta} \frac{F_V}{M_D} q_\gamma^\alpha p^\beta. \quad (42)$$

where  $M_D$  is the mass of  $D^0$  and the form factors are given by Eqs. (16) and (17).

Similar to the decays discussed in the previous subsection, we also define  $x_\gamma = 2E_\gamma/M_D$  and  $y = 2E_{\bar{\nu}}/M_D$  in the  $D$ -meson rest frame in order to re-scale the energies of the

photon and anti-neutrino. By integrating the variable  $y$  in the phase space, we obtain the differential decay rate of  $D^0 \rightarrow \nu \bar{\nu} \gamma$  as

$$\frac{d\Gamma}{dx_\gamma} = 2\alpha \left( \frac{G_F \alpha}{16\pi^2 \sin^2 \theta_W} \right)^2 (|F_A|^2 + |F_V|^2) \sum_{i=d,s,b} |V_{ui} V_{ci}^*|^2 D^2(x_i) x_\gamma^3 (1 - x_\gamma) M_D^5, \quad (43)$$

where we have included the three generations of neutrinos.

Using  $m_c = 1.4 \text{ GeV}$ ,  $m_u = 300 \text{ MeV}$ , and  $\omega = 0.5$ , the differential decay branching ratio  $dB(D^0 \rightarrow \nu \bar{\nu} \gamma)/dx_\gamma$  as a function of  $x_\gamma = 2E_\gamma/M_D$  is shown in Figure 5 and the integrated decay branching ratio is

$$B(D^0 \rightarrow \nu \bar{\nu} \gamma) = 2.7 \times 10^{-16}. \quad (44)$$

It is easy to see that in the standard model the branching ratio of  $D^0 \rightarrow \nu \bar{\nu} \gamma$  is too small to be measured experimentally. However, a large branching ratio may be induced by new physics such as the leptoquark model [19].

## 5 $D^0 \rightarrow l^+ l^- \gamma$

### 5.1 Matrix elements and kinematics

The contribution to the process of  $D^0 \rightarrow l^+ l^- \gamma$  ( $l = e$  or  $\mu$ ) arises from the effective Hamiltonian that induces the pure leptonic mode of  $D^0 \rightarrow l^+ l^-$ . The short distance contribution for  $c \rightarrow u l^+ l^-$  comes from the  $W$ -box,  $Z$ -boson and photon penguin diagrams, and the effective Hamiltonian is given by

$$\begin{aligned} \mathcal{L} = & -\frac{G_F \alpha}{2\sqrt{2}\pi \sin^2 \theta_W} \sum_{i=d,s,b} V_{ui} V_{ci}^* \left\{ F_i^1 \bar{u} \gamma_\mu P_L c \bar{l} \gamma^\mu (1 - \gamma_5) l + F_i^2 \bar{u} \gamma_\mu P_L c \bar{l} \gamma^\mu (1 + \gamma_5) l \right. \\ & \left. - 2 \frac{F_i^3 \sin^2 \theta_W}{p^2} m_c \bar{u} i \sigma_{\mu\nu} p^\nu P_R c \bar{l} \gamma^\mu l \right\}, \end{aligned} \quad (45)$$

where  $P_{L,R} = (1 \mp \gamma_5)/2$ , and  $p$  is the momentum transfer which is equal to the momentum of the lepton pair. The Wilson coefficients  $F_i^1, F_i^2, F_i^3$  can be found in Refs. [18, 20] and one has

$$\begin{aligned} F_i^1 &= C_i^1 + C_i^2 - \sin^2 \theta_W (C_i^3 + 2C_i^2), \\ F_i^2 &= -\sin^2 \theta_W (C_i^3 + 2C_i^2), \\ F_i^3 &= -Q \left( \left[ -\frac{1}{4} \frac{1}{x_i - 1} + \frac{3}{4} \frac{1}{(x_i - 1)^2} + \frac{3}{2} \frac{1}{(x_i - 1)^3} \right] x_i - \frac{3}{2} \frac{x_i^2 \ln x_i}{(x_i - 1)^4} \right) \\ &+ \left[ \frac{1}{2} \frac{1}{x_i - 1} + \frac{9}{4} \frac{1}{(x_i - 1)^2} + \frac{3}{2} \frac{1}{(x_i - 1)^3} \right] x_i - \frac{3}{2} \frac{x_i^3 \ln x_i}{(x_i - 1)^4}, \end{aligned} \quad (46)$$

where  $x_i = m_i^2/M_W^2$  with  $m_i$  ( $i = d, s, b$ ) being the current quark masses. The coefficients of  $C_i^1$ ,  $C_i^2$  and  $C_i^3$  are given by

$$\begin{aligned}
C_i^1 &= \frac{3}{8} \left[ -\frac{1}{x_i - 1} + \frac{x_i \ln x_i}{(x_i - 1)^2} \right] - \gamma(\xi, x_i), \\
C_i^2 &= \frac{x_i}{4} - \frac{3}{8} \frac{1}{x_i - 1} + \frac{3}{8} \frac{2x_i^2 - x_i}{(x_i - 1)^2} \ln x_i + \gamma(\xi, x_i), \\
C_i^3 &= Q \left( \left[ \frac{1}{12} \frac{1}{x_i - 1} + \frac{13}{12} \frac{1}{(x_i - 1)^2} - \frac{1}{2} \frac{1}{(x_i - 1)^3} \right] x_i \right. \\
&\quad + \left[ \frac{2}{3} \frac{1}{x_i - 1} + \left( \frac{2}{3} \frac{1}{(x_i - 1)^2} - \frac{5}{6} \frac{1}{(x_i - 1)^3} + \frac{1}{2} \frac{1}{(x_i - 1)^4} \right) x_i \right] \ln x_i \Big) \\
&\quad - \left[ \frac{7}{3} \frac{1}{x_i - 1} + \frac{13}{12} \frac{1}{(x_i - 1)^2} - \frac{1}{2} \frac{1}{(x_i - 1)^3} \right] x_i \\
&\quad - \left[ \frac{1}{6} \frac{1}{x_i - 1} - \frac{35}{12} \frac{1}{(x_i - 1)^2} - \frac{5}{6} \frac{1}{(x_i - 1)^3} + \frac{1}{2} \frac{1}{(x_i - 1)^4} \right] x_i \ln x_i - 2\gamma(\xi, x_i), \quad (47)
\end{aligned}$$

and

$$\begin{aligned}
\gamma(\xi, x_i) &= \frac{1}{\xi x_i - 1} \left( \frac{3}{4} \frac{1}{x_i - 1} + \frac{1}{8} \frac{1}{\xi x_i - 1} \right) x_i \ln x_i - \frac{1}{8} \frac{1}{\xi} \frac{1}{\xi x_i - 1} \\
&\quad \times \left[ \left( \frac{5\xi + 1}{\xi - 1} - \frac{1}{\xi x_i - 1} \right) \ln \xi + 1 \right], \quad (48)
\end{aligned}$$

where  $\xi$  is a gauge dependent parameter. The decay amplitude for  $D^0 \rightarrow l^+ l^- \gamma$  can be written as

$$\mathcal{M}(D^0 \rightarrow l^+ l^- \gamma) = \mathcal{M}_{IB} + \mathcal{M}_{SD} \quad (49)$$

where  $\mathcal{M}_{IB}$  and  $\mathcal{M}_{SD}$  represent the  $IB$  and  $SD$  contributions, respectively. For the  $IB$  part, the amplitude is clearly proportional to the lepton mass  $m_l$  and it can be written as:

$$\mathcal{M}_{IB} = -ie \frac{G_F \alpha}{2\sqrt{2}\pi \sin^2 \theta_W} \sum_{i=d,s,b} V_{ui} V_{ci}^* f_D m_l (F_i^2 - F_i^1) \left[ \bar{l} \left( \frac{\not{\epsilon} \not{P}_D}{2p_1 \cdot q_\gamma} - \frac{\not{P}_D \not{\epsilon}}{2p_2 \cdot q_\gamma} \right) \gamma_5 l \right], \quad (50)$$

where  $P_D$ ,  $p_1$ ,  $p_2$  and  $q_\gamma$ , are the momenta of  $D$ ,  $l^+$ ,  $l^-$  and photon respectively. The amplitude for the  $SD$  part, where a photon is from the initial quark line, is given by

$$\begin{aligned}
\mathcal{M}_{SD} &= -\frac{G_F \alpha}{2\sqrt{2}\pi \sin^2 \theta_W} \sum_{i=d,s,b} V_{ui} V_{ci}^* \left\{ F_i^1 \langle \gamma(q_\gamma) | \bar{u} \gamma_\mu P_L c | D(p + q_\gamma) \rangle \bar{l} \gamma^\mu (1 - \gamma_5) l \right. \\
&\quad + F_i^2 \langle \gamma(q_\gamma) | \bar{u} \gamma_\mu P_L c | D(p + q_\gamma) \rangle \bar{l} \gamma^\mu (1 + \gamma_5) l \\
&\quad \left. - 2 \frac{F_i^3 m_c \sin^2 \theta_W}{p^2} \langle \gamma(q_\gamma) | \bar{u} i \sigma_{\mu\nu} p^\nu P_R c | D(p + q_\gamma) \rangle \bar{l} \gamma^\mu l \right\}, \quad (51)
\end{aligned}$$

which shows that to find the decay rate, one has to evaluate the hadronic matrix elements in Eq. (51).

Using Eqs. (2) and (3), we rewrite Eqs. (51) as:

$$\begin{aligned} \mathcal{M}_{SD} = & \frac{G_F \alpha}{2\sqrt{2}\pi \sin^2 \theta_W} \sum_{i=d,s,b} V_{ui} V_{ci}^* \left\{ \epsilon_{\mu\alpha\beta\sigma} \epsilon^{*\alpha} p^\beta q_\gamma^\sigma \left[ A \bar{l} \gamma^\mu l + C \bar{l} \gamma^\mu \gamma_5 l \right] \right. \\ & \left. + i \left[ \epsilon_\mu^* (p \cdot q_\gamma) - (\epsilon^* \cdot p) q_{\gamma\mu} \right] \left[ B \bar{l} \gamma^\mu l + D \bar{l} \gamma^\mu \gamma_5 l \right] \right\}, \end{aligned} \quad (52)$$

where the factors of  $A$ - $D$  are

$$\begin{aligned} A &= \frac{(F_i^1 + F_i^2)}{M_D} F_{VA}(p^2) - 2 F_i^3 \frac{m_c}{p^2} F_{TA}(p^2), \\ B &= \frac{(F_i^1 + F_i^2)}{M_D} F_{VV}(p^2) - 2 F_i^3 \frac{m_c}{p^2} F_{TV}(p^2), \\ C &= \frac{(F_i^2 - F_i^1)}{M_D} F_{VA}(p^2), \\ D &= \frac{(F_i^2 - F_i^1)}{M_D} F_{VV}(p^2), \end{aligned} \quad (53)$$

respectively.

## 5.2 Decay rates

The partial decay width for  $D^0 \rightarrow l^+ l^- \gamma$  in the  $D^0$  rest frame is found to be:

$$d\Gamma = \frac{1}{2M_D} |\mathcal{M}|^2 (2\pi)^4 \delta(P - p_1 - p_2 - q_\gamma) \frac{d\vec{q}}{(2\pi)^3 2E_\gamma} \frac{d\vec{p}_1}{(2\pi)^3 2E_1} \frac{d\vec{p}_2}{(2\pi)^3 2E_2}, \quad (54)$$

where the square of the matrix element is given by

$$|\mathcal{M}|^2 = |\mathcal{M}_{IB}|^2 + |\mathcal{M}_{SD}|^2 + 2\text{Re}(\mathcal{M}_{IB} \mathcal{M}_{SD}^*). \quad (55)$$

To describe the kinematics of  $D^0 \rightarrow l^+ l^- \gamma$ , we define two variables of  $x_\gamma = 2P_D \cdot q_\gamma / M_D$  and  $y = 2P_D \cdot p_1 / M_D$ . We write the transfer momentum  $p^2$  in term of  $x_\gamma$  as:

$$p^2 = M_D^2 (1 - x_\gamma). \quad (56)$$

The double differential decay rate is then found to be:

$$\frac{d^2 \Gamma^l}{dx_\gamma d\lambda} = \frac{M_D}{256\pi^3} |M|^2 = C \rho(x_\gamma, \lambda), \quad (57)$$

where

$$C = \alpha \sum_{i=d,s,b} \left| \frac{\alpha V_{ui} V_{ci}^*}{8\pi^2} \right|^2 G_F^2 M_D^5 \quad (58)$$

and

$$\rho(x_\gamma, \lambda) = \rho_{IB}(x_\gamma, \lambda) + \rho_{SD}(x_\gamma, \lambda) + \rho_{IN}(x_\gamma, \lambda), \quad (59)$$

with

$$\begin{aligned}
\rho_{IB} &= 4|f_D(F_i^2 - F_i^1)|^2 \frac{r_l}{M_D^2 x_\gamma^2} \left\{ \frac{x_\gamma^2 - 2x_\gamma + 2 - 4r_l}{\lambda(1 - \lambda)} - 2r_l \left( \frac{1}{\lambda^2} + \frac{1}{(1 - \lambda)^2} \right) \right\}, \\
\rho_{SD} &= \frac{M_D^2}{8} x_\gamma^2 \left\{ (|A|^2 + |B|^2) \left[ (1 - x_\gamma + 2r_l) - 2(1 - x_\gamma)(\lambda - \lambda^2) \right] \right. \\
&\quad + (|C|^2 + |D|^2) \left[ (1 - x_\gamma - 2r_l) - 2(1 - x_\gamma)(\lambda - \lambda^2) \right] \\
&\quad \left. + 2\text{Re}(B^*C + A^*D)(1 - x_\gamma)(2\lambda - 1) \right\}, \\
\rho_{IN} &= f_D(F_i^2 - F_i^1) r_l \left\{ \text{Re}(A) \frac{x_\gamma}{\lambda(1 - \lambda)} + \text{Re}(D) \frac{x_\gamma(1 - 2\lambda)}{\lambda(1 - \lambda)} \right\}. \tag{60}
\end{aligned}$$

Here  $\lambda = (x_\gamma + y - 1)/x_\gamma$  and  $r_l = m_l^2/M_D^2$  and the physical regions for  $x_\gamma$  and  $\lambda$  are given by:

$$\begin{aligned}
0 &\leq x_\gamma \leq 1 - 4r_l, \\
\frac{1}{2} - \frac{1}{2} \sqrt{1 - \frac{4r_l}{1 - x_\gamma}} &\leq \lambda \leq \frac{1}{2} + \frac{1}{2} \sqrt{1 - \frac{4r_l}{1 - x_\gamma}}. \tag{61}
\end{aligned}$$

In Figure 6 we present the differential decay rate of  $D^0 \rightarrow \mu^+ \mu^- \gamma$  as functions of  $x_\gamma$ . From the figures we see that the contributions from soft photons, *i.e* the IB ones, corresponding to small  $x_\gamma$  region, are infrared divergence. To obtain the decay width of  $D^0 \rightarrow l^+ l^- \gamma$ , a cut on the photon energy is needed. The integrated branching ratios are summarized in Table 3. Here, we have used the cut value of  $\delta = 0.01$  and  $m_c = 1.5 \text{ GeV}$ ,  $m_s = 0.4 \text{ GeV}$  and  $m_d = 0.3 \text{ GeV}$  in the calculations of the form factors. We have also used  $|V_{cd}V_{ud}^*| = |V_{cs}V_{us}^*| = 0.2145$ ,  $|V_{cb}V_{ub}^*| = 1.6 \times 10^{-4}$ ,  $\tau(D^0) = 0.415 \times 10^{-12} \text{ s}$  [16] to evaluate the numerical results.

Table 3: Integrated branching ratios for the radiative leptonic  $D^0$  decays

Integrated Decay Branching Ratios	IB	SD	IN	Sum
$10^{11} B(D^0 \rightarrow e^+ e^- \gamma)$	$1.3 \times 10^{-9}$	6.3	$4.6 \times 10^{-4}$	6.3
$10^{11} B(D^0 \rightarrow \mu^+ \mu^- \gamma)$	$1.9 \times 10^{-5}$	6.3	$2.2 \times 10^{-3}$	6.3

We see that the decay branching ratios of the radiative leptonic decays of  $D^0 \rightarrow l^+ l^- \gamma$  are about eight orders of magnitude larger than that of the purely leptonic modes of  $D^0 \rightarrow l^+ l^-$  for  $l = e$  and  $\mu$ , respectively.

## 6 Conclusions

We have calculated the form factors of the  $D \rightarrow \gamma$  within the light-front model and used these form factors to evaluate the branching ratios of the leptonic  $D$ -meson radiative decays. We have found that, in the standard model, the decay branching ratios of  $D_{(s)}^+ \rightarrow e^+ \nu_e \gamma$ ,  $D_{(s)}^+ \rightarrow \mu^+ \nu_\mu \gamma$  and  $D_{(s)}^+ \rightarrow \tau^+ \nu_\tau \gamma$  are  $6.9 \times 10^{-6}$  ( $7.7 \times 10^{-5}$ ),  $2.5 \times 10^{-5}$  ( $2.6 \times 10^{-4}$ ), and  $6.0 \times 10^{-6}$  ( $3.2 \times 10^{-4}$ ), and that of  $D^0 \rightarrow l^+ l^- \gamma$  ( $l = e, \mu$ ) and  $D^0 \rightarrow \nu \bar{\nu} \gamma$  are  $6.3 \times 10^{-11}$  and  $2.7 \times 10^{-16}$ , respectively. Comparing with the purely leptonic decays of  $D^0 \rightarrow l^+ l^-$ , we have found that the rates of the corresponding radiative modes are several orders of magnitude larger. We conclude that some of the radiative leptonic decays could be measured in the BTeV/C0 experiment at Fermilab [21]. During Tevatron Run II, which could reconstruct about  $10^9$  charm mesons decays and increase the upper limit of about three orders.

## Acknowledgments

This work was supported in part by the National Science Council of the Republic of China under contract numbers NSC-89-2112-M-007-013 and NSC-89-2112-M-006-026.

## References

- [1] I.I. Bigi, CERN-TH. 7370/94, (1994).
- [2] E791 Collaboration, E. M. Aitala *et la.*, Phys. Rev. Lett. **76**, (1996) 364.
- [3] E771 Collaboration, T. Alexopoulos *et la.*, Phys. Rev. Lett. **77**, (1996) 2380;.
- [4] CLEO Collaboration, A. Freyberger *et la.*, Phys. Rev. Lett. **76**, (1993) 3065.
- [5] S. L. Glashow, J. Iliopoulos and L. Maiani, Phys. Rev. **D2**, 1285 (1970).
- [6] Chi-Yee Cheung, Wei-Min Zhang and Guey-Lin Lin, Phys. Rev. **D52**, 2915 (1995).
- [7] Wei-Min Zhang, Chin. J. Phys. **31**, 717 (1994).
- [8] K. G. Wilson, T. Walhout, A. Harindranath, W. M. Zhang, R. J. Perry and S. Glazek  
Phys.Rev. **D49** (1994) 6720-6766
- [9] Hai-Yang Cheng, Chi-Yee Cheung and Chien-Wen Hwang, Phys. Rev. **D55**, 1559  
(1997).
- [10] M. Terent'ev, Sov. J. Phys. **24**, 106 (1976); V. Berestetsky and M. Terent'ev, *ibid*  
**24**, 547 (1976); **25**, 347 (1977); P. Chung, F. Coester and W. Polyzou, Phys. Lett.  
**B205**, 545 (1988).
- [11] W. Jaus, Phys. Rev. **D41**, 3394 (1990); **44**, 2851 (1991); P. J. O'Donnell and Q. P.  
Xu, Phys. Lett. **B325**, 219; **336**, 113 (1994).
- [12] G. Burdman, T. Goldman, and D. Wyler, Phys.Rev. **D51**, 111 (1995).
- [13] D. Atwood, G. Eilam and A. Soni Mod. Phys. Lett. **A11**, 1061 (1996).
- [14] Gregory P. Korchemsky, Dan Pirjol and Tung-Mow Yan, Phys.Rev. **D61** (2000)  
114510.
- [15] C. Q. Geng, C. C. Lih, and Wei-Min Zhang, Phys. Rev. **D57**, 5697 (1998); C. C.  
Lih, C. Q. Geng and W. M. Zhang, Phys. Rev. **D59** (1999) 114002.
- [16] Particle Data Group, Eur. Phy. Soc. J. **C3**, 1 (1998).
- [17] C. Bernard, Nucl. phys. **B34** (Proc. Suppl.) 47 (1994).
- [18] Takeo Inami and C. S. Lim, Prog. Theor. Phys. **65** (1981) 297.



- [19] C. Q. Geng, Z. Phys. **C48** (1990) 279.
- [20] A. J. Schwartz, Mod. Phys. Lett. **A8** (1993) 967.
- [21] D. Kaplan, e-print hep-ex 9705002.

## Figure Captions

- Figure 1: The values of the form factors  $F_V$  (solid curve) and  $F_A$  (dashed curve) as functions of the momentum transfer  $p^2$  for  $D_s^+ \rightarrow \gamma$ .
- Figure 2: The values of the form factors  $F_{TV}$  (solid curve) and  $F_{TA}$  (dashed curve) as functions of the momentum transfer  $p^2$  for  $D_s^+ \rightarrow \gamma$ .
- Figure 3: The differential decay branching ratio  $dB(D^+ \rightarrow \mu^+ \nu_\mu \gamma)/dx_\gamma$  as a function of  $x_\gamma = 2E_\gamma/M_D$ .
- Figure 4: The differential decay branching ratio  $dB(D_s^+ \rightarrow \mu^+ \nu_\mu \gamma)/dx_\gamma$  as a function of  $x_\gamma = 2E_\gamma/M_{D_s}$ .
- Figure 5: The differential decay branching ratio  $dB(D^0 \rightarrow \nu \bar{\nu} \gamma)/dx_\gamma$  as a function of  $x_\gamma = 2E_\gamma/M_D$ .
- Figure 6: The differential decay branching ratio  $dB(D^0 \rightarrow \mu^+ \mu^- \gamma)/dx_\gamma$  as a function of  $x_\gamma = 2E_\gamma/M_D$ .

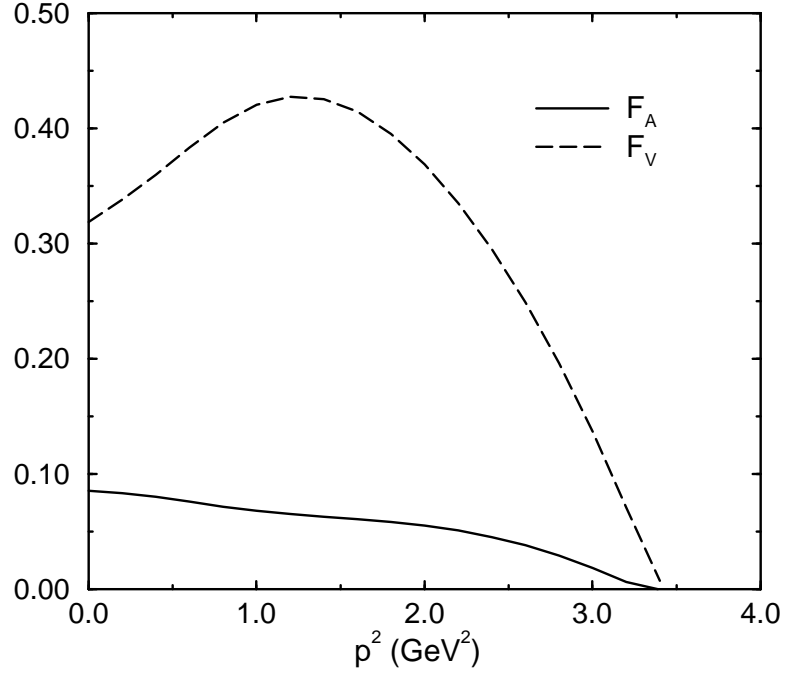


Figure 1: The values of the form factors  $F_A$  (solid curve) and  $F_V$  (dashed curve) as functions of the momentum transfer  $p^2$  for  $D_s^+ \rightarrow \gamma$ .

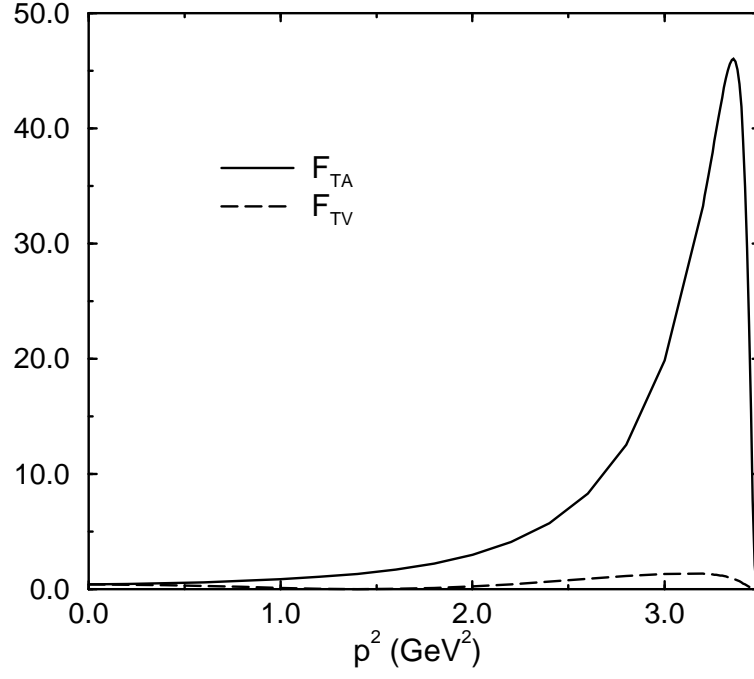


Figure 2: The values of the form factors  $F_{TA}$  (solid curve) and  $F_{TV}$  (dashed curve) as functions of the momentum transfer  $p^2$  for  $D_s^+ \rightarrow \gamma$ .

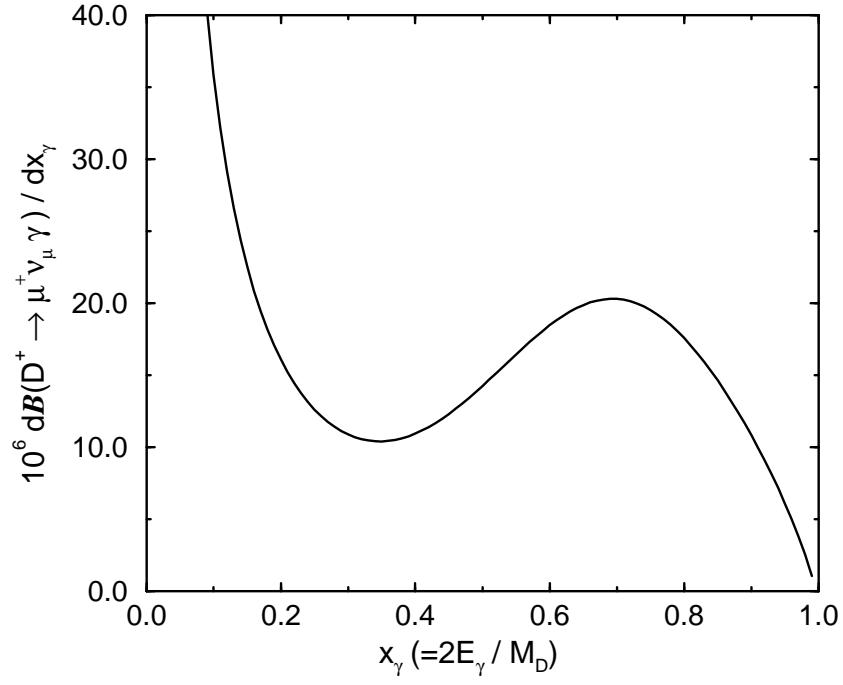


Figure 3: The differential decay branching ratio  $dB(D^+ \rightarrow \mu^+ \nu_\mu \gamma)/dx_\gamma$  as a function of  $x_\gamma = 2E_\gamma/M_D$ .

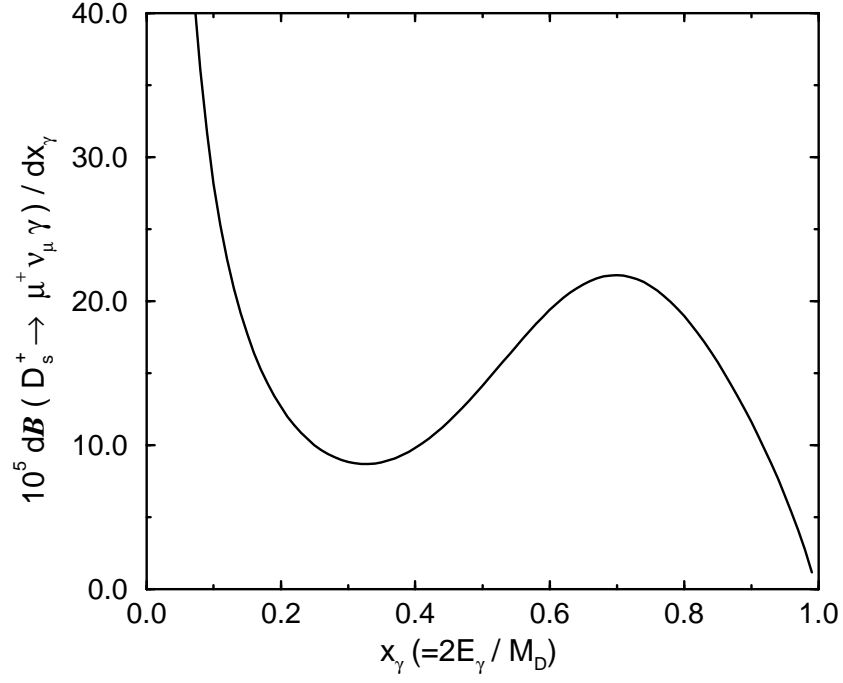


Figure 4: The differential decay branching ratio  $dB(D_s^+ \rightarrow \mu^+ \nu_\mu \gamma)/dx_\gamma$  as a function of  $x_\gamma = 2E_\gamma/M_D$ .

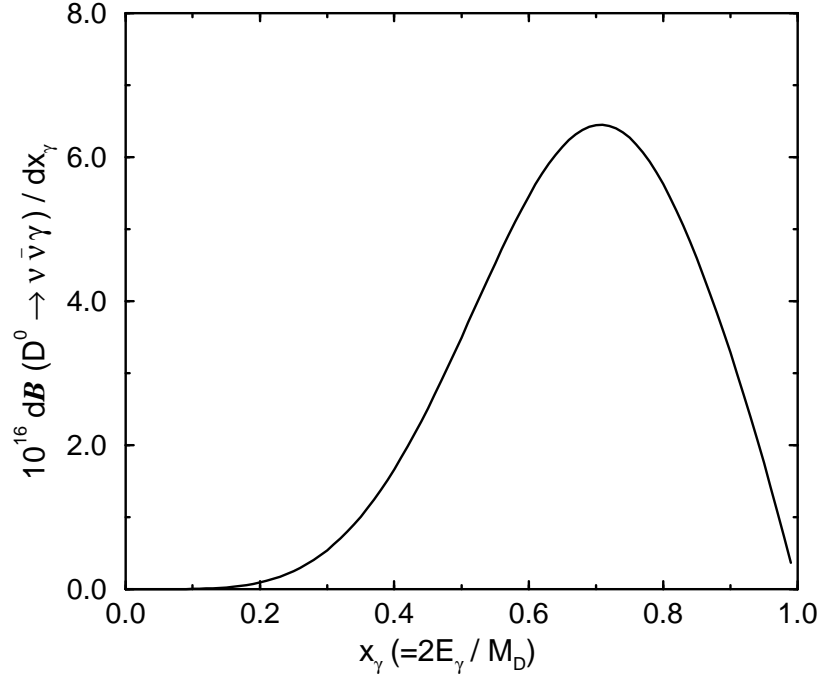


Figure 5: The differential decay branching ratio  $dB(D^0 \rightarrow \nu \bar{\nu} \gamma)/dx_\gamma$  as a function of  $x_\gamma = 2E_\gamma/M_D$ .

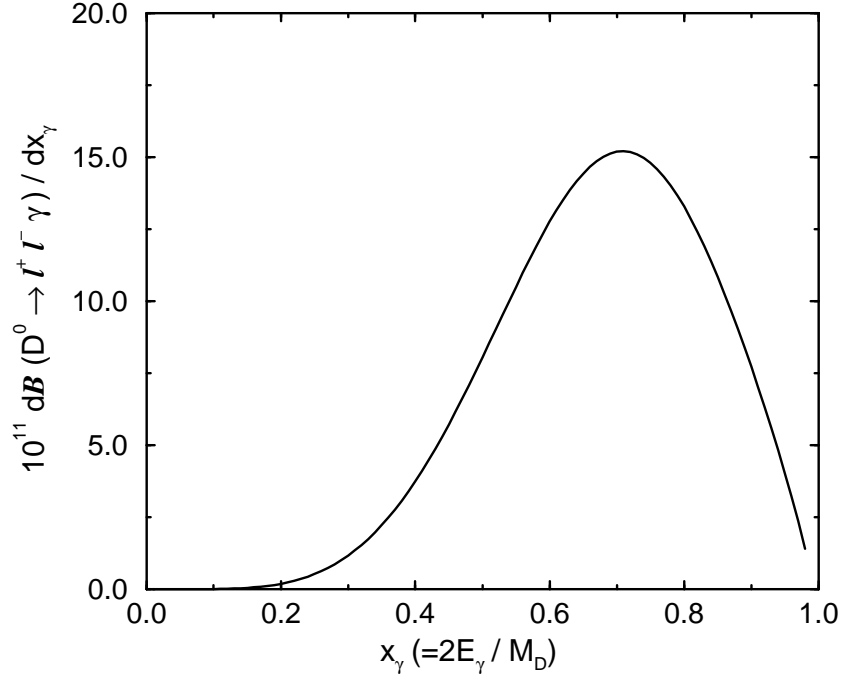


Figure 6: The differential decay branching ratio  $dB(D^0 \rightarrow \mu^+ \mu^- \gamma)/dx_\gamma$  as a function of  $x_\gamma = 2E_\gamma/M_D$ .